مجلة

كلية التـــراث الجامعة

مجلة علمية محكمة

متعددة التخصصات نصف سنوية

العدد التاسع والثلاثون

عدد خاص بوقائع المؤتمر العلمي السنوي السادس عشر (الدولي الخامس)

18 نيسان 2024

ISSN 2074-5621

رقم الايداع في دار الكتب والوثائق 719 لسنة 2011

مجلة كلية التراث الجامعة معترف بها من قبل وزارة التعليم العالي والبحث العلمي بكتابها المرقم (ب 3059/4) والمؤرخ في (4/7 /2014)

Calculation of UMP and Effects of Broken Bars Location on Performance Electrical Machine

Khaleel J. Hammadi

Abstract
The unbalanced magnetic pull UMP is the resultant global magnetic force that acts on the rotor due to an asymmetric magnetic field distribution in the air gap as broken rotor bars condition. It can be computed by normally found during finite element analysis using Maxwell's stress method. In this paper, influence of the broken bars location upon the amplitudes of current waveform is investigated. The stator current frequency spectrum, waveform flux density, variations of torque for a faulted induction motor are obtained for all cases in which four broken bars are distributed over poles of the motor. The torque frequency spectrum of faulted motor has been obtained for various cases of bars breakage location.

هو القوة المغناطيسية الناتجة التي تعمل على الدوار بسبب توزيع المجال UPM السحب المغناطيسي غير المتوازن [1] المغناطيسي غير المتماثل في فجوة الهواء كحالة قضبان الدوار المكسورة. يمكن حسابها عن طريق العثور عليها أثناء تحليل العناصر المحدودة باستخدام طريقة الإجهاد ماكسويل. في هذا البحث تم دراسة تأثير موقع القضبان المكسورة على سعة شكل موجة التيار. يتم الحصول على طيف تردد تيار الجزء الثابت، وكثافة تدفق الشكل الموجي، وتغيرات عزم الدوران للمحرك التعريفي المعيب لجميع الحالات التي يتم فيها توزيع أربعة قضبان مكسورة على أقطاب المحرك. تم الحصول على طيف تردد عزم الدوران للمحرك المعطل في حالات مختلفة من مواقع كسر القضبان.

Keywords: UMP; broken rotor bars; faults diagnosis; induction motors;

I. Introduction

Fault diagnosis methods are widely utilized for maintenance and protection of induction motors. The principle of any reliable fault recognition technique is steady-state analysis of electrical, magnetic and mechanical behavior of the motor under fault conditions; modeling is the first step for studying this phenomenon. The FE method enables one to calculate the magnetic field distribution within the motor using its exact geometry and magnetic characteristics. Knowing the magnetic field distribution, other quantities of the motor such as variations stator current waveform, air gap magnetic flux density and different inductances can be obtained [1]. A finite element coupled method has been used to analyze and diagnose a faulty induction motor [2] .Modeling of the motor to simulate performance of the faulty motor, selection of proper signal for processing and feature extraction are necessary. The technique that has been used over many years for mechanical fault diagnosis is based on the temperature and vibration changes [3].However; it is clear that electrical signals such as stator current can be used for the same purpose. Particularly, processing stator current spectrum for diagnosis of the rotor faults such as broken rotor bars and eccentricity has been widely used [4]. In fact, stator current is the most convenient signal for fault diagnosis; the reasons are its sensitivity to the fault, availability of suitable sensors from the quality and cost point of views, capability of considering the fault conditions in the model, capability of the model in computation of the chosen signal variations against fault conditions and finally fault severity have a unique influence upon the signal characteristics. To this end, the stator current spectra are analyzed to detect different kinds of faults [5]. In [6] and [7], magnitude of side band components at frequencies around the supply frequency in the stator current spectrum has been used as a criterion for broken rotor bar. In [8] and [9], magnitude of the side band components at frequencies around the principal slot harmonic has been employed to detect different types of eccentricities. In many published papers for diagnosis and analysis of broken rotor bars of induction motor, current of the broken bars is taken to be zero, while this means considerable increase of current in the bars adjacent to the broken bars [10] and [11].

Table I :Squirrel-cage induction motor parameters

Number of poles	4
Number of phases	3
Outer diameter of stator	140mm
Inner diameter of stator	76mm
Air gap length	0.6mm
Axial length	52mm
Number of stator slots	24
Number of rotor bars	24
Rated voltage (V) rms	320
Rated frequency (Hz)	50
Number of stator turns/phase	150

In Table 1, I show the specifications of proposed motor used in this study. The torque frequency spectrum of a faulted induction motor has been obtained for various cases of the bars breakage location and shown that the bars breakage location influences the amplitudes of harmonic components in the torque frequency [12]. It is indicated that the location of the rotor bars has significant effect upon the torque of the faulty motor and waveform flux density distribution in air gap .when the broken bars concentrate over one pole of the motor comparison with another location, the torque of faulty motor oscillates more. Now make comparison between different cases for distribution of broken bars under poles and discussion what happen for motor component.

In this modeling, we discuss geometrical and characteristics of all parts of the motor and effected distribution of location broken bars over different poles of the motor at the current stator and another components due to the fault, spatial distribution of stator windings, field distribution and flux density concentration.

II. Based Of Magnetic Field Analysis

Magnetic field waveform contains full information about the stator and rotor positions and mechanical parts of the motor. Distribution of the magnetic flux density is calculated from the magnetic potential vector A as follows [13]:

$$B = \nabla \times A \qquad (1)$$

Based on the Maxwell stress method, the stress tensor applied to the rotor surface is as follows:

$$T = \frac{B_n^2 - B_t^2}{2\mu_0} \qquad (2)$$

where B_n=radial tangential components

B_t=tangential components of the magnetic flux density.

μ_0=permeability of free space= $4\pi 10^{-7}$

The electromagnetic torque is determined by integration of T over the stator and rotor surface:

$$T_{em} = \frac{r_0 l}{\mu_0} \oint B_n B_t \, ds \qquad (3)$$

where T_{em}= the electromagnetic torque

μ_0=permeability of free space= $4\pi 10^{-7}$

l= axial length

In a healthy induction motor, the stator rotating field and rotor rotating field develops a uniform torque. In a faulty motor, a field opposite to the stator main field induces current in the rotor; this interacts with the rotor main flux and develops a torque with twice slip frequency, this increases the noise and slip and the torque oscillation frequency is increased by increase of the load. Although in all cases, the frequency of torque variation is equal to the twice slip frequency. Asymmetry of stator and rotor increases the stator harmonics current, torque variations, temperature rise; mean torque decreases and losses increase which leads to a lower efficiency and asymmetrical magnetic flux distribution has been used to diagnose the broken rotor bars. These signs and some of their secondary signs can be used as indexes for fault diagnosis of the motor. So far, for detection of these indexes, various methods have been proposed which cover different aspects of science and technology. Different cases for distribution of broken bars under poles with full load and same speed motor, and the influence of the broken bars location and concentration of broken bars on one pole upon the performance of the faulty motor is investigated.

III. Case One

The effected location has four broken bars over one pole of the motor as shown in Figure 1a. In this case, it is shown the influence of broken bars location and concentration it on one pole upon the performance of the faulty motor on stator current, torque, waveform flux density are a very high effective comparison with healthy motor. Figure 1b shows the magnetic flux distribution with broken bars. The number of broken bars can lead to a more asymmetry in the flux density distribution in air-gapFigure1d; Figure 1c presents time variations of stator current for healthy motor and motor with broken rotor bar. Presents the time variations of torque for a healthy and faulty induction motor with four broken bars, Comparison in Figure7, indicates that the rotor broken bars increases the oscillation of the developed torque when motor under load and low speed.

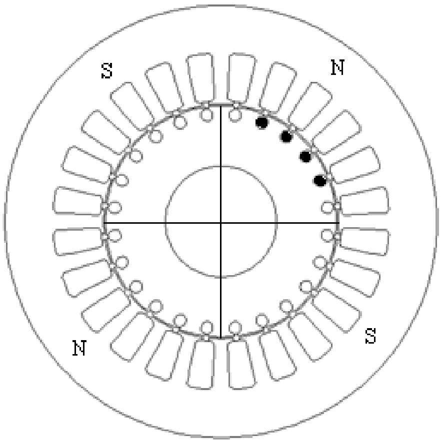

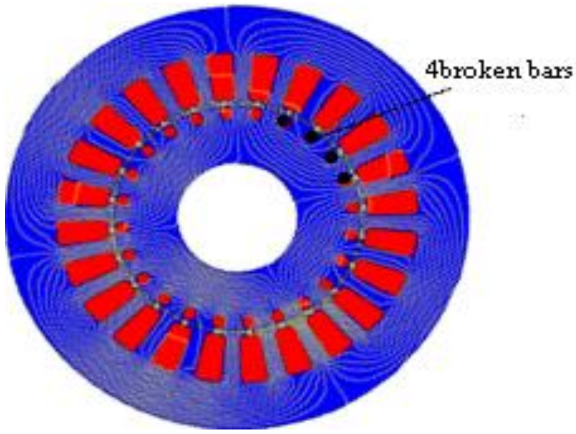

(a) **(b)**

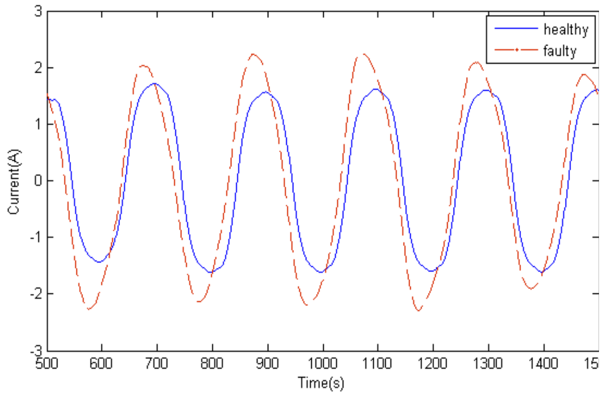

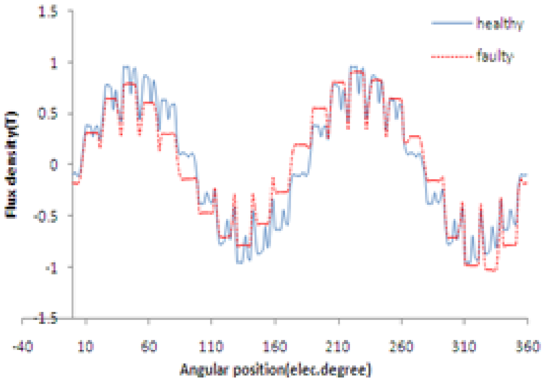

(c) **(d)**

Figure 1 (a) distribution of four broken bars under one pole (b) Magnetic flux distribution (c) Time variations of current in healthy motor and motor with four broken bars(d) waveform flux density distribution in air gap induction motor

Figure 2 shows the stator current frequency spectrum for four broken bars under one pole. As it can see, the sidebands frequency harmonics can be observed in the figure. The most important harmonics caused by the broken rotor bars are as follows:

$$f_{BB}=((1\pm 2Ks)f_s) \qquad (4)$$

where s is slip of motor, f_s is supply frequency and K = 1, 2, 3, … These harmonics must be searched around the fundamental frequency component.

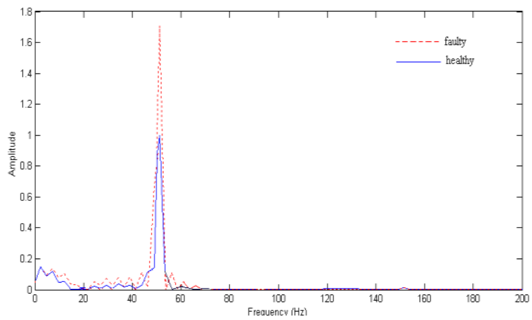

Figure2 Current spectrum of an induction motor with healthy and faulty state with 4 broken bars above one pole

Figure 3a shows the harmonic spectrum air gap flux density in healthy state and harmonic spectrum air gap flux density in faulty state.

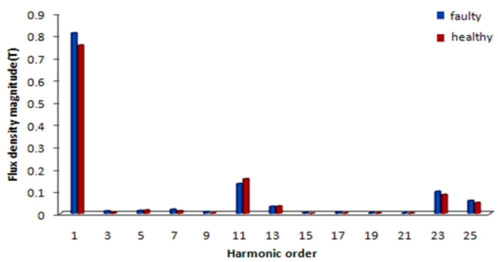

Figure3 Harmonic spectrum air gap flux density in healthy state and faulty state broken bars

IV. CASE TWO

In this case the distribution of the location four broken bars over two pole of the motor as shown in Figure 4a, it is shown the influence of broken bars location and concentration of broken bars on two poles upon the performance of the faulty motor on torque, waveform flux density is less than effective comparison with case one. Figure4b showed the flux density distribution in air-gap. Presents the time variations of torque for a healthy and faulty condition as shows in figuer7, Comparison with case1 indicates that the location rotor broken bars a few increases the oscillation of the developed torque.

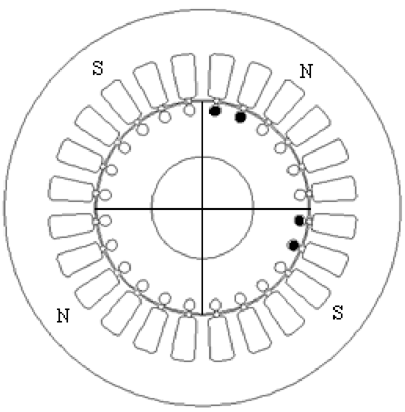

(a)

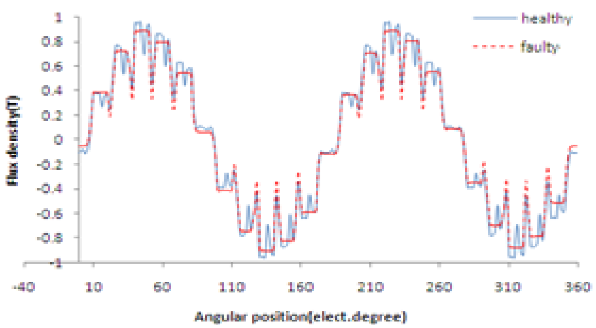

(b)

Figure4 (a) distribution of broken bars under two pole (b) waveform flux density distribution in air gap induction motor

V. Case Three

In this case the distribution of the location two broken bars over one pole and another two broken on opposite pole of the motor Figure 5a, it is shown the influence of broken bars location and concentration of broken bars on two poles upon the performance of the faulty motor on torque, waveform flux density is less than effective comparison with case one.Figure5b shown the flux density distribution in air-gap. Presents the time variations of torque for a healthy and faulty induction motor with four broken bars as shows in figure7, Comparison in case1 indicates that the location rotor broken bars also a few increases the oscillation of the developed torque.

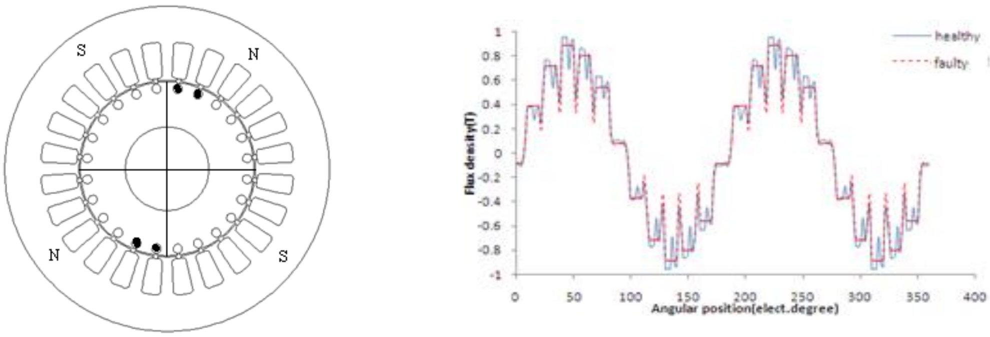

(a) **(b)**

Figure5 (a) distribution of broken bars under two opposite pole (b) waveform flux density distribution in air gap induction motor

VI. Case Four

In this case the distribution of the location one broken bar one each pole of the motor Figure 6a, it is shown the influence of broken bars location and concentration of broken bars on four poles, upon the performance of the faulty motor on torque, waveform flux density is less than effective comparison with another case. Figure6b shown the flux density distribution in air-gap, Presents the time variations of torque for a healthy and faulty induction motor with four broken bars as shows in figure7, Comparison in case1 indicates that the location rotor broken bars also a few increases the oscillation of the developed torque.

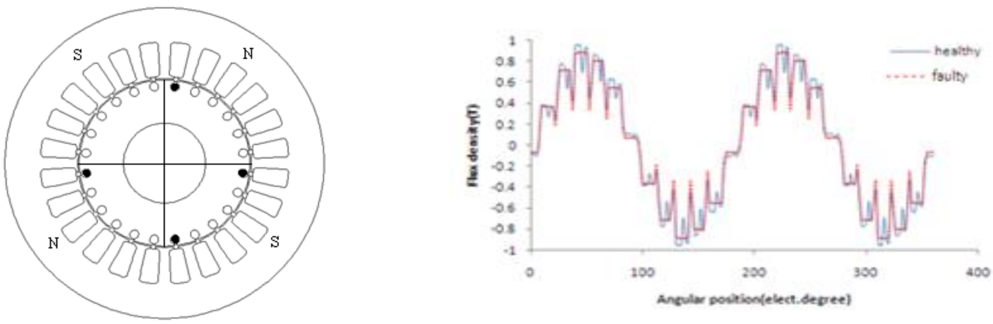

(a) **(b)**

Figure6 (a) distribution of broken bars under four poles (b) waveform flux density distribution in air gap induction motor

VII. Torque For The Case Of Rotor Conditions

Here, the developed torque profile are given in Figure7.Similarly, by comparison of all cases, one can notice the torque increased in the case when location broken rotor bars concentration over one pole. Furthermore, the computed average value of the torque, we notice that the developed torque for all cases depended of location of broken bars regarding of pole in motor.

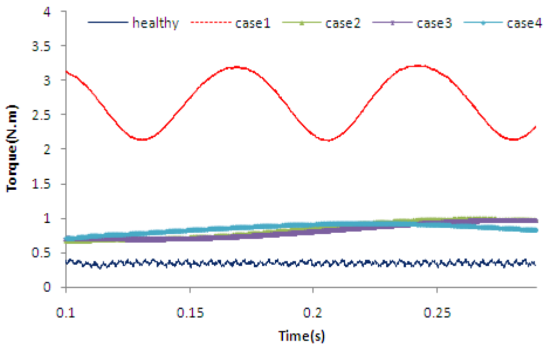

Figure7 Time variations torque with four broken bar location cases over pole.

VIII. Unbalanced Magnetic Pull

The unbalanced magnetic pull is the resultant global magnetic force that acts on the rotor due to an asymmetric magnetic field distribution in the air gap as broken rotor bars condition are given in figure8. It can be computed by finite element analysis using Maxwell's stress tensor method. The force components F_x and F_y which act on a rotor having an axial length l_a can be computed by evaluating the following expressions along a surface of radius r in the middle of air gap;

$$F_x = \frac{rl\alpha}{2\mu_0}\int_0^{2\pi}[(B_\alpha^2 - B_r^2)\cos\alpha + 2B_rB_\alpha\sin\alpha]d\alpha \quad (5)$$

$$F_y = \frac{rl\alpha}{2\mu_0}\int_0^{2\pi}[(B_\alpha^2 - B_r^2)\cos\alpha + 2B_rB_\alpha\cos\alpha]d\alpha \quad (6)$$

where F_x= force component on axial x
F_y= force component on axial y
l_a= axial length
B_α=circumferential flux density components
B_r= Radial flux density components

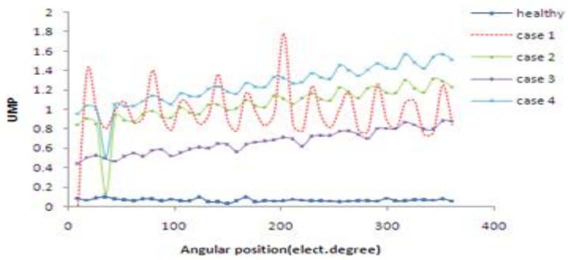

Figure 8 Output relationships between location broken rotor bars and UMP

IX. Influence Of Broken Bars Location On Induction Motor Performance

Table1 is explain the values of the output relationship between location broken rotor bars, rang amplitude of current , mid air gap flux density, average of torque and unbalanced magnetic pull.

In faulty motor, many harmonics components are injected into the stator current. Amplitudes of the time variations of current components are increased by increase of the fault percentage. In this paper, influence of the broken bars location upon the amplitudes of harmonics was investigated. Therefore, for signal processing of the stator current of the healthy and faulty motor, spectrum analysis of the stator current signal is necessary. It is notice that the amplitudes of harmonics due to broken bars placed on one pole are larger than the in case which the broken bars are distributed on four poles. Also in all cases presents the time variations of torque and waveform flux density for a faulty induction motor with four broken bars are depended of the location broken bars over poles when taken in account with another cases.

Table 1 Output relationship between location broken rotor bars and motor condition

Induction motor condition	Location of broken bars	Current in RMS value (A)	THD% Of the current	Average torque (N.m)	Average value of UMP (N)	Torque ripple
Healthy case	Healthy	1.27	40.45%	0.4	0	1.875
Faulty Case1	4 broken bars on 1 pole	1.69	34.88%	2.5	88.4	0.4
Faulty Case2	3 broken bars on 1 pole and 1broken bar on adjacent pole	1.06	39.34%	0.7	67.6	1.143
Faulty Case3	2 broken bars on 1pole and 2 broken bars on adjacent pole	1.272	39.80%	0.6	36.4	1.333
Faulty Case4	1 broken bar on each pole	1.20	39.18%	0.75	78	1.046

Conclusions

In this work Influence of broken rotor bars location on induction motor performance under four broken bars fault was modeled very precisely and with minimum simplifying assumptions using FEM. This modeling provided accessibility to the stator current signal very accurately. Component of the current and waveform flux density distribution in air gap induction motor was used to precisely diagnose the fault and depended on location of the broken bars. It was shown that the distribution of the broken bars over different poles increases the amplitude of the current components. It was shown that the broken bars increase the oscillation of the developed torque of the motor and stator current, waveform flux density when four broken bars are concentrated on one pole. It was proved that the location of the rotor bars has considerable effect on the performance and concentration of the broken bars on one pole of the motor increases the motor oscillation.

References

[1] Tsoumas I, Mitronikas E, Safacas A. Induction motor mixed fault diagnosis based on wavelet analysis of the current space vector. In: Proceedings of 8th international conference on electrical machines and systems, September 2015; p. 2186–91

[2] S. Nandi, H.A. Toliyat and Xiaodong Li, Condition monitoring and fault diagnosis of electrical motors – a review, IEEE Trans Energy Convers 20 (4) (2018), pp. 719–729.

[3] H. Calis and A. Cakir, Experimental study for sensorless broken bar detection in induction motors, J Energy Convers Manage 49 (April) (2010), pp. 854–862.

[4] H. Calis and A. Cakir, Experimental study for sensorless broken bar detection in induction motors, J Energy Convers Manage 49 (April) (2006), pp. 854–862.

[5] D.F. Pires, V.F. Pires, J.F. Martins and A.J. Pires, Rotor cage fault diagnosis in three-phase induction motors based on a current and virtual flux approach, J Energy Convers Manage 50 (2019), pp. 1026–1032.

[6] J.F. Bangura, R.J. Povinelli, N.A.O. Demerdash and R.H. Brown, Diagnostics of eccentricities and bar/end-ring connector breakages in poly phase induction motors through a combination of time series data mining and time-stepping coupled FE-state-space techniques industry applications, IEEE Trans Ind Appl 39 (4) (2020), pp. 1005–1013.

[7] B. Akin, U. Orguner, H.A. Toliyat and M. Rayner, Low order PWM inverter harmonics contributions to the inverter-fed induction machine fault diagnosis, IEEE Trans Ind Electron 55 (2) (2008).

[8] X. Li, Q. Wu and S. Nandi, Performance analysis of a three-phase induction machine with inclined static eccentricity, IEEE Trans Ind Appl 43 (2007), pp. 531–541.

[9] A. Ghoggal, S.E. Zouzou, H. Razik, M. Sahraouri and A. Khezzar, An improved model of induction motors for diagnosis purpose-slot skewing effect and air-gap eccentricity faults, J Energy Convers Manage 50 (February) (2009), pp. 1336–1347.

[10] Workshop in Design and modeling of electrical machine, school of electrical & electronic engineering USM Engineering campus March-2009 By Engr. DR. Dahaman isahak.

[11] R. Fiser, Application of a finite element method to predict damage induction motor performance, IEEE Trans Magn 37 (5) (2001), pp. 3635–3639.

[12] Faiz Jawad and Ebrahimi Bashir Mahdi, Locating rotor broken bars in induction motors using finite element method, J Energy Convers Manage **50** (2020), pp. 125–131.

[13] B. Akin, U. Orguner, H.A. Toliyat and M. Rayner, Low order PWM inverter harmonics contributions to the inverter-fed induction machine fault diagnosis, IEEE Trans Ind Electron 55 (2) (2008).